

Research Article

Fluoride Removal in Water Using Kaolin and Eggshell Powder Blend Adsorbents

Gayan Senarathna^{1*}, Dakshika Wanniarachchi¹, Saranga Diyabalanage S.²

¹Department of Chemistry, Faculty of Graduate Studies, University of Kelaniya, Kelaniya, Sri Lanka

²Instrument Center, University of Sri Jayewardenepura, Nugegoda, Sri Lanka

E-mail: gayansenarathna77@gmail.com

Received: 15 May 2024; **Revised:** 26 August 2024; **Accepted:** 30 August 2024

Abstract: Fluoride contamination in water has emerged as a significant global concern due to its adverse health effects when consumed in excess. This study is focused on developing an eco-friendly, cost-effective adsorbent for fluoride removal using eggshells and kaolin. Adsorbent blends were prepared by mixing kaolin and eggshell powder in six different ratios, namely; 100:0, 80:20, 65:35, 50:50, 35:65, and 20:80. Cylindrical-shaped pellets were produced from each of the blends and subjected to the thermal treatment at 950 °C. Fluoride adsorption capacities of the pellets were investigated at different pH conditions (from pH 2 to pH 10) for a 5 mg/L fluoride solution with 1 g of adsorbent dosage and 60 min of contact time. Pellets with a 50:50 ratio (CKE₃) were found to be the most effective adsorbent considering the adsorption capacity and stability at all the studied pH conditions. At pH 6, CKE₃ showed an adsorption capacity of 0.06 mg/g compared to 0.02 mg/g of kaolin-only pellets. XRD, TGA-DSC, EDX and SEM analysis were used to characterize the adsorbent. XRD analysis showed that the raw adsorbent contained phases of CaCO₃ and kaolinite, whereas the calcined material comprised Ca(OH)₂ and metakaolinite. Batch experiments were carried out with CKE₃ for adsorbent dosage, pH, contact time, and initial fluoride concentration. An adsorbent dosage of 4 g was capable of resulting in a 53% removal of fluoride for a 5 mg/L solution after 60 min of contact time. Pseudo-first-order and pseudo-second-order kinetic models were applied in the study, and pseudo-second-order exhibited the best fit. The isotherm data were studied for Langmuir and Freundlich models, and the results were satisfactorily fitted with Langmuir isotherm.

Keywords: adsorption, fluoride removal, eggshell, kaolin

1. Introduction

Fluoride is one of the most significant chemicals in water because of its impact on human health. Just like a double-edged sword, fluoride has beneficial effects on teeth at low concentrations and, in turn, causes detrimental health effects such as fluorosis when consumed at excessive levels. Human exposure to fluorides can occur through drinking water, dental products, food, beverages and fluoride-contaminated air due to cases such as coal burning, production of phosphate fertilizers, and volcanic activity. However, drinking water is the largest and most prominent route of fluoride exposure, and it is responsible for about 75% of daily fluoride intake¹.

Natural sources are the primary cause of fluoride contamination in drinking water, and some anthropogenic activities may also contribute a considerable proportion². Geogenic processes including weathering, dissolution, and pedogenic

processes associated with fluoride-bearing minerals and fluoride-rich soils are the major natural causes of the leaching of fluorides into groundwater^{3,4}. Volcanic eruptions and marine aerosols are the other two potential natural sources of fluoride contamination⁵. Industrial activities such as the steel industry, ceramics industry, phosphate fertilizer processing, aluminium industry, combustion of coal, non-ferrous metal foundries and agricultural activities such as phosphate fertilizer application (superphosphate, potash, and NPK fertilizer) and pesticides application are possible anthropogenic sources of fluoride contamination in drinking water^{6,7}.

The spatial distribution of fluoride in groundwater is mainly encountered by the underlying geology around the world other than hydrological and anthropogenic factors. Elevated fluoride concentrations are reported globally in more than 25 countries, including those mainly in Asia, Africa, North America, Latin America, and Europe². More than 200 million people worldwide depend on consuming water contaminated with high fluoride levels, and the majority are reported from Asia and Africa⁴.

Consumption of low fluoride concentrations between 0.5 mg/L to 1.0 mg/L is beneficial for preventing dental caries⁸. World Health Organization (WHO) has set a guideline value of 1.5 mg/L for fluorides in drinking water. However, excessive exposure may lead to fluorosis, which is a condition caused by irreversible demineralization of tooth tissues and bones. Depending on the dose and duration of exposure, this can range from mild dental fluorosis to crippling skeletal fluorosis⁹.

Various techniques are used for de-fluoridation such as coagulation/precipitation methods, membrane processes, ion-exchange processes and adsorption processes. Adsorption is the widely used process amongst all the other methods for defluoridation of water because of its cost-effectiveness, ease of operation, high removal capacities and sustainable usage. A variety of adsorbents has been studied in previous studies including alumina and aluminium-based adsorbents, clays and clay minerals, carbon-based adsorbents, calcium-based adsorbents, layered double hydroxides, natural materials (i.e., chitosan, zeolite, chitin, algae, collagen), building material/industrial waste adsorbents, agricultural and biomass-based adsorbents, and nano-sorbents¹⁰⁻¹³. The latest studies have been focused on developing adsorbents by integrating two or more adsorbent materials to enhance the adsorption efficiencies¹⁴⁻¹⁶. Activation of materials by acid treatment^{17,18}, thermal treatment¹⁹ and mechanochemical treatment²⁰ are applied in the process of adsorbent material development. In addition, some materials such as clays and biomass-based materials have been chemically modified in order to enhance adsorption capacities^{16,21-25}. The use of natural materials as adsorbents has been a novel practice for fluoride removal in water because of their salient features such as sustainability, lack of interferences and cost-effectiveness. In this study, a kaolin and eggshell powder blend was developed as the adsorbent material for fluoride removal in water.

Kaolin is a clay material which contains kaolinite [$\text{Al}_2\text{Si}_2\text{O}_5(\text{OH})_4$] mineral as the major constituent and some other minerals such as illite and quartz in minor percentages^{26,27}. The chemical composition of kaolin is mainly composed of SiO_2 and Al_2O_3 ²⁸. Moreover, components such as Fe_2O_3 , CaO , MgO , TiO_2 , and K_2O could be found in minor percentages^{26,27}. Clays are considered to be effective adsorbents due to the properties they possess such as higher surface area, molecular sieve structure, ion exchange potential, chemical and mechanical stability and various structural properties. Also positively charged surface of clay minerals makes them more affinitive to negatively charged ions¹². Kaolin consists of aluminium and silica which are major constituents in many adsorbents used in previous studies which have shown significant adsorption capacities^{14,15,17,22,29,30}. Moreover, kaolin contains hydroxide ions which are capable of ion exchange with fluoride ions²⁷. In literature, several studies on kaolin are available which have shown the potential of using kaolin as an adsorbent for defluoridation of water^{18,20,27}.

The eggshell is the solid protective cover of the egg which consists of three layers namely; Cuticle (outermost layer), Testa (Calcium carbonate middle layer) and Mammillary layer (innermost layer). These layers are formed with numerous pores in a manner to facilitate water transpiration and air exchange in the shell³¹. An eggshell consists of about 94% of calcium carbonate, 1% calcium phosphate, 1% of magnesium carbonate, and 4% of organic components³². The presence of many pores and calcium as the main constituents makes eggshells promising for fluoride removal in potable water^{19,32}. Eggshell powder has been studied for fluoride removal in some studies and has shown effective adsorption capacities³³⁻³⁵. Furthermore, eggshell powder has been incorporated with other potential adsorbents and studied for fluoride removal^{15,36,37}.

However, the capability of a kaolin and eggshell powder blend adsorbent for fluoride removal in water has not been studied so far. Hence, this study is focused on developing an adsorbent incorporating these two materials into calcined pellets. Calcination may enhance the adsorption capacity of eggshell powder¹⁹ and optimize the usability of kaolin²⁸.

In most of the studies, adsorption studies are carried out with the powdered form of the adsorbent. However, the use of powdered adsorbent may cause plenty of inconveniences such as filtration issues when it comes to practical scenarios. Also in column studies, powders may cause high pressure drop, column blockage and low flow rate²⁸. Therefore, in this study, the adsorbent was formulated in pellet form, and investigations were conducted on fluoride removal efficiency, kinetics, and isotherms.

2. Materials and methods

2.1 Materials and chemicals

White chicken eggshells were obtained from local cafeterias. Kaolin powder was obtained from the Meetiyaoda kaolin refinery in Sri Lanka. Sodium Fluoride (Fisher Scientific, assay—99%), SPANDS-Sodium2-(parasulfophenylazo)-1,8-dihydroxy-3,6-naphthalene disulfonate (HACH, assay—99.9%) and Zirconyl Chloride Octahydrate (Sigma-Aldrich, assay—98%) were obtained in reagent grade.

2.2 Eggshell powder and kaolin powder blend preparation

White chicken eggshells were cleaned thoroughly several times with water to remove any contaminants. The inner membranes of the shells were peeled off and washed with distilled water. Cleaned shells were air-dried and then oven-dried at 105 °C for 24 h. The dried shells were cooled down in a desiccator. They were ground to a fine powder and then sieved through a 250 µm sieve.

The kaolin powder was oven-dried at 105 °C until a constant weight was achieved. After cooling, the dried kaolin was sieved through a 250 µm sieve. Eggshell powder and kaolin powder were weighed separately to create mixtures in six different ratios: 100:0, 80:20, 65:35, 50:50, 35:65, and 20:80. Pellets were then prepared from each set of blends. These prepared pellets were oven-dried at 105 °C for 2 h to remove moisture, followed by calcination at 950 °C for 4 h (Table 1).

Table 1. Adsorbent blends and the kaolin eggshell percentages

Adsorbent	Kaolin and Eggshell Powder Percentage	
	Kaolin %	Eggshell Powder %
Blank	100	-
CKE ₁	80	20
CKE ₂	65	35
CKE ₃	50	50
CKE ₄	35	65
CKE ₅	20	80

2.3 Adsorbent characterization

The mineralogical characterizations of raw sample (RKE₃), calcined sample (CKE₃) and kaolin-only blank were done using X-ray diffraction (XRD; Rigaku Ultima IV), in the 2 theta angle range of 5° to 80°. Thermo gravimetric analysis (TGA) with differential scanning calorimetry (DSC) was performed for raw sample (RKE₃) using thermogravimetric analyzer (TA-SDT 65). Surface morphology of CKE₃, RKE₃ and fluoride adsorbed material (ACKKE₃) was investigated using Scanning Electron Microscope (SEM, CARL ZEISS EVO 18), while composition was examined by Energy Dispersive X-ray Spectroscopy (EDX).

2.4 Optimization of kaolin-eggshell composite

A stock fluoride solution of 100 mg/L was prepared using anhydrous sodium fluoride (NaF). A solution of 5 mg/L NaF was prepared by diluting the 100 mg/L stock solution.

Each of the blends was analyzed for fluoride adsorption capacity keeping the adsorbent dose (1 g), contact time (1 h), initial fluoride concentration (5 mg/L) and pH constant (5.7). Experiments were done in 250 mL glass conical flasks using 50 mL portions of 5 mg/L fluoride solution. Fluoride concentrations of the initial and final solutions were analyzed by APHA SPADNS Method³⁸. Dilutions were made whenever needed.

Adsorption capacity was calculated using Equation (1).

$$\text{Adsorption Capacity } (q) = \frac{(C_o - C_t)}{W} \times V \quad (1)$$

where q is the amount of F^- adsorbed per unit gram of the adsorbent t (mg/g), C_o is the initial fluoride concentration (mg/L), C_t is the fluoride concentration at time t (mg/L), V is the volume of fluoride solution (L) and W is the mass of adsorbent.

Then; CKE₁, CKE₂, CKE₃ and CKE₄ pellets were studied for adsorption capacity and stability at different pH conditions (2, 4, 6, 8, 10) keeping the adsorbent dose (1 g), contact time (1 h) and initial fluoride concentration (5 mg/L) constant. HCl and NaOH (0.1 N) solutions were used to adjust the pH and were measured using a calibrated pH meter (Apera PH 9500). Pellets having the 50:50 kaolin and eggshell ratio (CKE₃) were found to be the best material concerning the adsorption capacity and stability of the pellets at all pH conditions tested.

2.5 Adsorption studies

Adsorption studies were carried out with CKE₃ for contact time, adsorbent dose, pH, and initial concentration. All experiments were done in 250 mL glass conical flasks and using 50 mL portions of 5 mg/L fluoride solution. The percent removal and adsorption capacity were calculated.

Percent removal of fluoride was calculated using the Equation (2)

$$\% \text{ Fluoride removal} = \frac{(C_o - C_f)}{C_o} \times 100 \quad (2)$$

where C_o and C_f are the initial fluoride concentration (mg/L) and final fluoride concentration (mg/L).

2.6 Kinetic studies

Kinetic study was carried out in 20 min time intervals of up to 2 h keeping dose (1 g), fluoride concentration (5 mg/L) and pH (5.7) constant at room temperature. The experiments were done in 250 mL conical flasks with 50 mL of F^- solution and conducted in triplicate. Pseudo-first-order and pseudo-second-order kinetic models were applied.

2.7 Isotherm studies

For isotherm studies, 50 mL portions of fluoride solutions with varying concentrations (1 mg/L, 2 mg/L, 3 mg/L, 4 mg/L and 5 mg/L) were analyzed keeping the adsorbent dosage (1 g), contact time (60 min) and pH (5.7) constant at room temperature. Experiments were triplicated. Langmuir model and Freundlich models were applied.

2.8 Quality analysis of the CKE₃-treated water sample

A 5 mg/L fluoride solution which was treated with 1 g of adsorbent for 1 h was analyzed for total hardness and Calcium content. APHA 2340 C method 100 was used for total hardness determination and a flame atomic photometer

(Jenway PFP7) was used for Calcium concentration analysis. Mitigation actions were taken to lower the residual calcium ion concentration by using pre-washed pellets for adsorption studies.

3. Results and discussion

3.1 Adsorbent characterization

Cylindrical-shaped adsorbent pellets were developed in this study. The calcined pellets were white in colour and a single pellet had an average weight, length and diameter of about 0.01 g, 3 mm and 1.5 mm respectively (Figure 1).

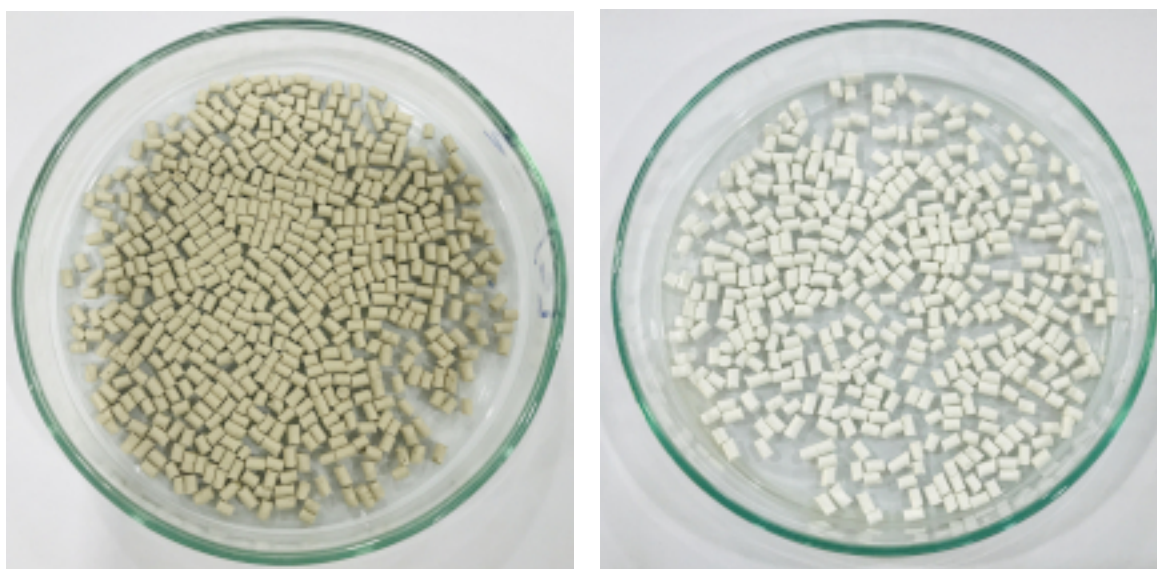


Figure 1. Images of (a) Raw pellets and (b) Calcined pellets

The XRD spectra of RKE₃ and CKE₃ are illustrated in Figures 2 and 3 respectively. The peaks in the RKE₃ spectrum at 2- θ values of 23.076, 29.467, 36.00, 39.462, 43.243, 47.202, 47.572, 48.561, 56.65, 57.466, 60.99, 64.46, 65.701, and 72.99 corresponded to calcite (S1, Supplementary Information). Since CaCO₃ (Calcite) is the major component of eggshells, these results confirm that the adsorbent contained eggshell powder³⁹. The peaks at 2- θ values of 18.01, 29.15, 34.15, 47.20, 50.84, and 54.28 in CKE₃ were aligned with portlandite (Ca(OH)₂) (S2, Supplementary Information). Therefore, it indicates that calcium carbonate present in RKE₃ has been decomposed into calcium oxide (CaO) evolving CO₂ in the process of calcination at 950 °C. However, calcium oxide has been converted to calcium hydroxide due to exposure to moisture in the atmosphere⁴⁰. The removal of amorphous organic components during calcination and phase transformation of calcite to portlandite enhance the overall crystallinity of the remaining material. Similar XRD results have been observed for eggshell powder in previous studies^{19,39,40}.

Furthermore, XRD peaks of RKE₃ observed at $2\theta = 12.409, 20.42, 24.888, 26.64, 35.25, 38.46$ corresponded to crystalline mineral phases of kaolin clay^{41–43}. This confirms that adsorbent was also composed of kaolin in addition to eggshells. Peaks of kaolinite were observed at $2\theta = 12.409, 20.42$ and 24.888 , while a quartz peak was observed at $2\theta = 26.64$ ^{41,42}. Therefore, it is clear that kaolinite is the major mineral phase of raw kaolin, while quartz has a minor presence. Peaks observed in CKE₃ at $2\theta = 28.030$ and 37.02 were attributed to calcined kaolin⁴⁴. However, in CKE₃, kaolinite characteristic peaks were found to be decreased when compared to that of raw kaolin. This shows that, due to thermal treatment, crystalline kaolinite has been transformed into an amorphous phase known as metakaolinite²⁶.

The XRD patterns of the blank sample which consisted only of calcined kaolin, showed more of an amorphous structure as shown in Figure 4. Only two distinct peaks were observed at $2\theta = 26.729$ and 45.9 . This reflects that, kaolinite in kaolin has been converted into amorphous metakaolinite after calcination⁴⁵. However, when comparing the XRD patterns of blank and CKE₃, it is very evident that the inclusion of eggshell powder has significantly raised the degree of crystallinity in the adsorbent.

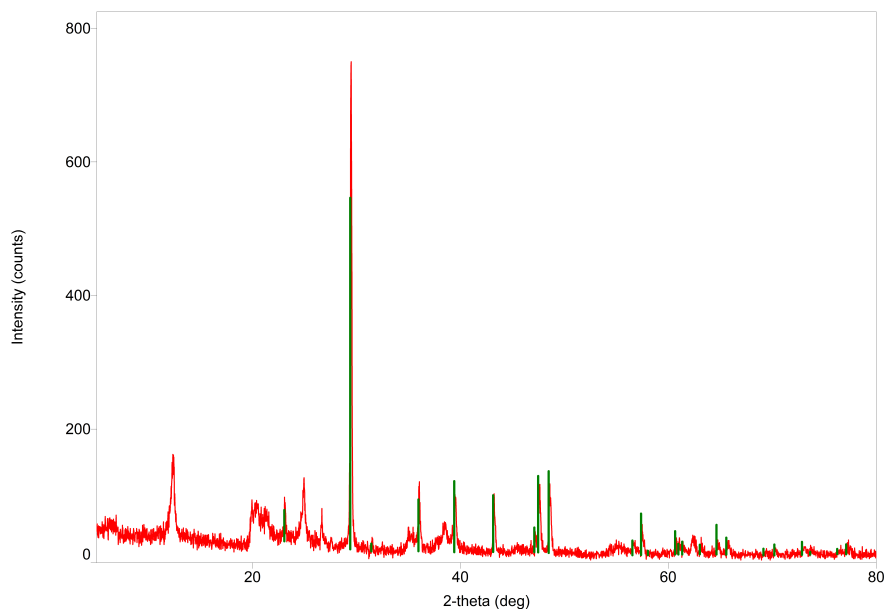


Figure 2. X-ray diffraction patterns of raw eggshell and kaolin-RKE₃

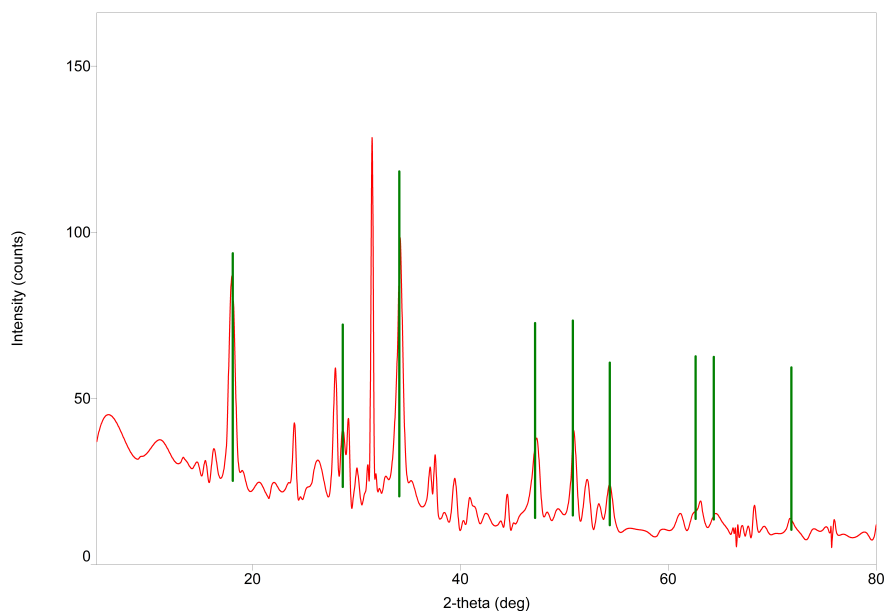


Figure 3. X-ray diffraction patterns of calcined eggshell and kaolin-CKE₃

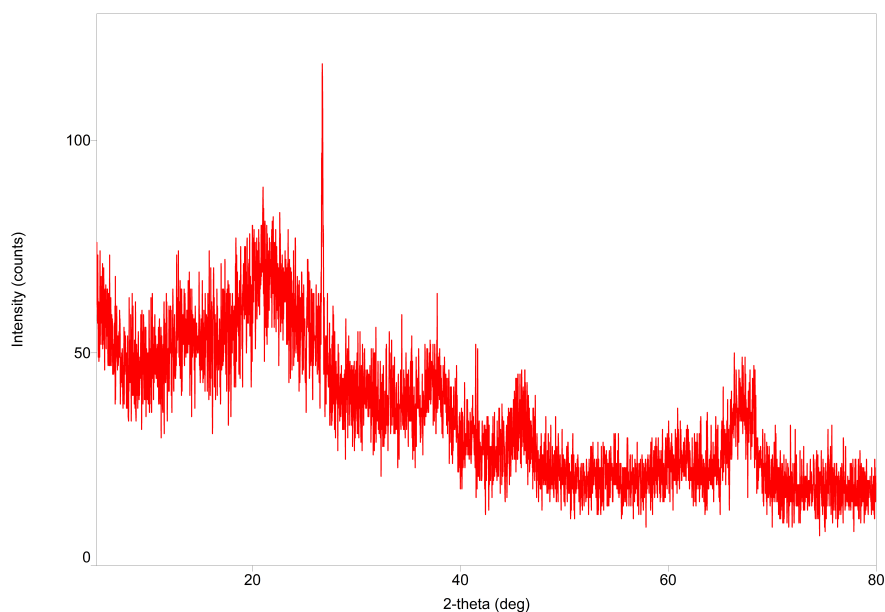
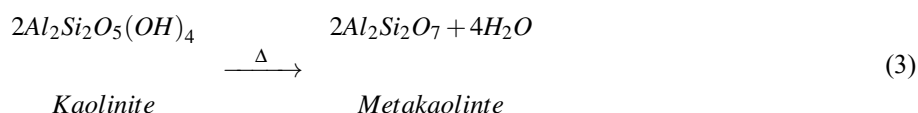


Figure 4. X-ray diffraction patterns of calcined kaolin-only blank

The TGA and DSC curves of the RKE₃ sample in the range of 26 °C to 900 °C are shown in Figure 5. The TGA pattern of RKE₃ showed three distinct stages of weight loss. The first region was a decreasing plateau from room temperature to 450 °C which gave an overall weight loss of about 5%. This was attributed to moisture and organic matter weight loss. From room temperature to 250 °C, the weight loss was due to the removal of moisture and surface-adsorbed water molecules³³. The next weight loss was about 5%, which took place between 450 °C to 650 °C. This mass loss could be due to the dehydroxylation of kaolinite in kaolin to form metakaolinite⁴⁶. The dehydroxylation process could have continued up to 750 °C²⁶. Between 500 °C and 750 °C, kaolinite loses its crystallographic order, as evidenced by the absence of Bragg scattering when heated above these temperatures⁴⁶. This transformation of kaolinite to amorphous metakaolinite by calcination was also confirmed by the XRD results.



In the third stage of the thermogram, a rapid weight loss of about 20% was observed from 650 °C to 750 °C. This is due to the emission of CO₂, resulting from the decomposition of CaCO₃ into CaO in eggshell powder¹⁹. This was also indicated by the structural changes in the XRD results. At 750 °C, a total weight loss of 31.41% was observed in the sample, where most of the weight loss had taken place after 650 °C. After 800 °C, the weight loss was almost constant, which depicts that the thermal decomposition of CaCO₃ was completed³².



Moreover, DSC analysis indicated an endothermic peak with a minimum at 740 °C which attributed to thermal decomposition CaCO₃³².

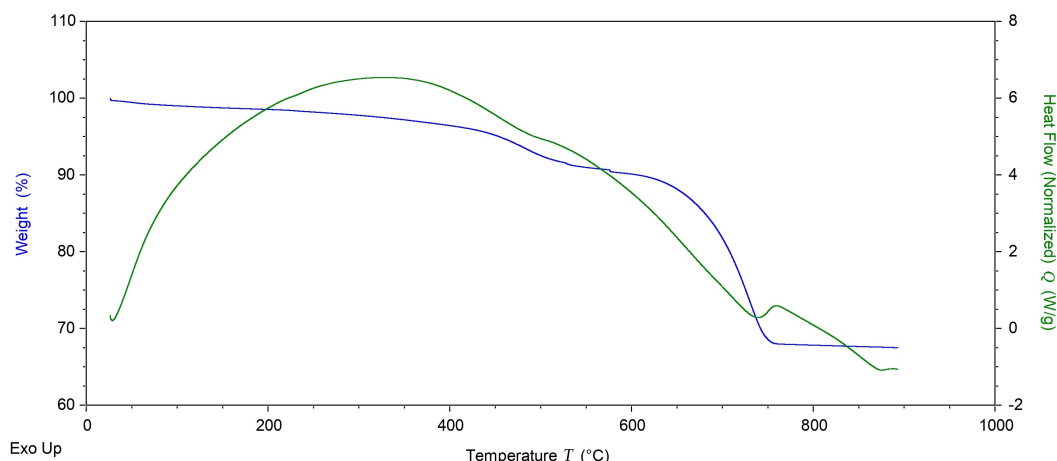


Figure 5. TGA-DSC analysis patterns of RKE₃ as a function of temperature

The EDX spectra of the raw adsorbent (RKE₃) is given S3 (Supplementary Material). The spectra illustrate the presence of elements: Carbon, Oxygen, Calcium, Aluminum and Silicon with weight percentages of 5.10%, 62.31%, 2.16%, 16.48, and 13.96% respectively. This confirms that adsorbent material consisted of kaolin, which is composed of SiO₂ and Al₂O₃ as main constituents and eggshell which is mainly composed of CaCO₃.

The surface morphologies of the raw adsorbent (RKE₃), calcined adsorbent (CKE₃) and fluoride adsorbed adsorbent (ACKE₃) obtained from SEM are given in S4 (Supplementary Material). The raw kaolin-eggshell (RKE₃) surface has a porous, irregular structure with evident micropores. Pores with diameters of less than 1 μm are observed in RKE₃. In order to facilitate the passage of gases from the inner to the outer side of the eggshell, eggshells naturally contain hollow pores that are created between the crystalline calcite crystals⁴⁷. After the thermal treatment at 950 °C, larger heterogeneous pores and cavities are observed in CKE₃. This might be due to the release of CO₂ gas with the conversion of CaCO₃ to CaO during calcination. In CKE₃ more pores are visible with larger diameters between 1–5 μm. Also, the surface texture has changed comparatively to a regular appearance. Kaolin has a layered structure and layer stripping occurs at higher temperatures⁴⁶. It is clearly observed that micro-cracks are present in CKE₃ because of calcination. The large heterogeneous pores and cavities provide a higher surface area for fluoride adsorption.

The fluoride-adsorbed kaolin-eggshell (ACKE₃) surface illustrates a regular, adhesive appearance as shown in S3 (Supplementary Material). The number of pores has decreased compared to that of CKE₃. This shows that fluoride adsorption has affected the orientation of the adsorbent particles. Bhaumik et al. and Jae-In Lee et al. have reported similar observations in studies done with eggshell powder^{19,34}.

3.2 Optimization of kaolin-eggshell composite

All six types of adsorbent pellets were studied for their fluoride adsorption capacity and material stability. It was observed that the adsorption capacity of the materials was increasing with the increasing percentage of eggshell powder in their composition. Several research studies have been conducted on the removal of fluoride from water, utilizing either eggshell powder or kaolin^{18,20,34,35}. However, the use of an integrated material of these two is not available in the literature. The results are clearly expressing that the eggshell powder is the key contributor to adsorption capacity. It also complies with the previous studies of water de-fluoridation, as studies on eggshell powder studies have reported higher adsorption capacities when compared to studies on kaolin.

CKE₅ was omitted for further selection studies since they were unstable and dissolved in water. So, in order to select the best out of CKE₁, CKE₂, CKE₃ and CKE₄, stability and adsorption capacity were evaluated at different pH conditions. The variation of adsorption capacities at different pH conditions are shown in Figure 6. CKE₄ demonstrated

higher adsorption capacities across all pH conditions, likely due to its higher percentage of eggshell powder. But, at pH 8 and pH 10, CKE₄ was observed to be unstable. Also, there was a considerable variation in the adsorption capacity of the CKE₄ pellets with varying pH when compared to other three. The percentage variation between the highest and lowest adsorption capacities was 38% for CKE₄, compared to 30% for CKE₃. Both CKE₂ and CKE₁ have shown lower adsorption capacities. Therefore, considering the stability and adsorption capacity of the pellets at different pH conditions, CKE₃ was chosen as the best adsorbent. Further studies were carried out with CKE₃.

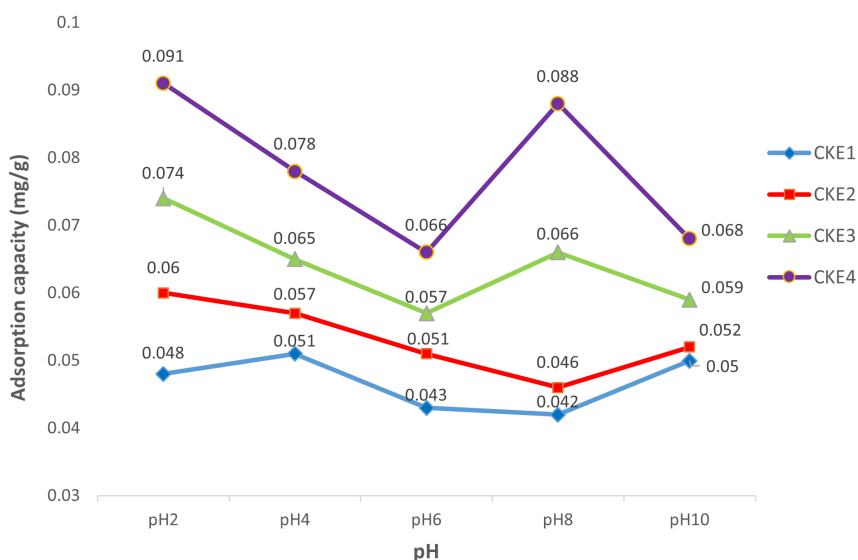


Figure 6. Comparison of the adsorption capacities of CKE₁, CKE₂, CKE₃ and CKE₄ at different pH conditions

3.3 Adsorption studies

3.3.1 Effect of contact time

The effect of contact time on fluoride adsorption for CKE₃ was evaluated with a concentration of 5 mg/L and an adsorbent dose of 1 g for a time period of 2 h. The graph of percent removal versus contact time is shown in Figure 7. The percent removal of fluoride was increased up to 22.2% in the first 60 min at a rapid rate and then slowed down to achieve an equilibrium in 100 min with a percent removal of 25.6%. The residual fluoride concentration after 60 min was 3.9 mg/L, and the minimum was reported to be 3.7 mg/L after 100 min. The rapid rate of adsorption in the initial phase is because of the higher availability of active binding sites on the surface of the adsorbent³⁴. The adsorption rate gradually slowed down due to the less availability of the active sites, lower fluoride concentration and repulsion of adsorbed fluoride ions onto the adsorbent surface^{36,48}. This reduction of adsorption sites might also indicate the formation of a monolayer of fluoride ions on the external surface of the adsorbent^{27,35}.

3.3.2 Effect of adsorbent dose

The effect of CKE₃ dose on fluoride adsorption was studied varying the mass from 0.5 g to 4.0 g. Figure 8 illustrates how the percent removal of fluorides varied with the increasing CKE₃ adsorbent dose. The removal percentage of fluoride increased with the increasing CKE₃ dose starting at a low percent removal of 13% at an adsorbent dose of 0.5 g. Maximum percent removal in the studied conditions was indicated as 53% at an adsorbent dose of 4.0 g. The percent removal of fluoride increases with the increasing adsorbent dose due to the increase of adsorbent surface area and availability of more active sites³⁰. Similar trends are observed in the previous studies on fluoride removal by kaolinite⁴⁹ and eggshells³³.

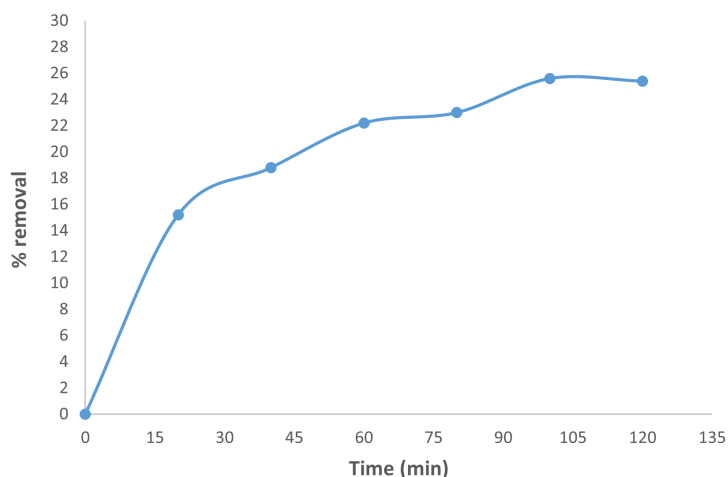


Figure 7. Effect of contact time on % removal of fluorides

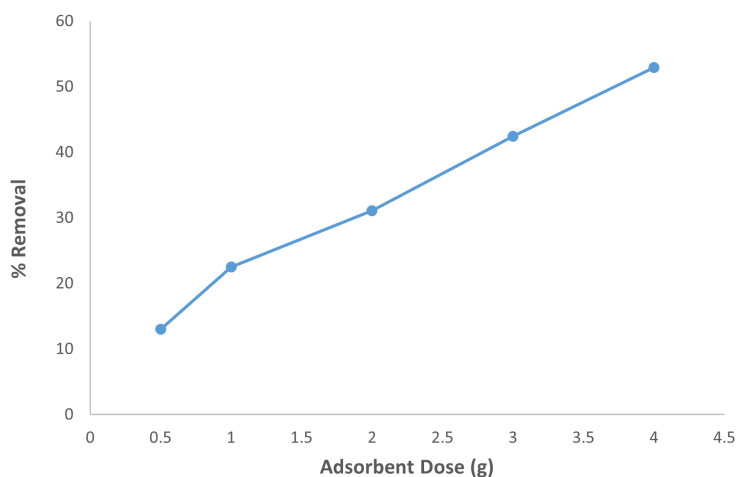


Figure 8. Effect of CKE₃ dose on % removal of fluorides

3.3.3 Effect of pH

The chemical and electrostatic interactions between the adsorbent surface and the fluoride ion and the availability of active sites on the adsorbent might be affected by the pH of the solution in fluoride adsorption⁵⁰. As shown in Figure 6, there was no significant variation in adsorption capacity across the different pH levels, indicating that CKE₃ is an effective adsorbent under all the pH conditions tested. This may be due to the composite nature of the material, which consists of several phases containing calcium, alumina and silica. Slight higher adsorption capacities at lower pH show that higher H⁺ concentration causes the adsorbent surface to be positively charged and hence favours the adsorption of negatively charged fluoride ions³⁰. Similar results were observed in separate studies which have used calcined eggshell powder¹⁹ and calcined kaolin²⁸. From pH 8 onwards adsorption capacity showed a gradual decrease with the increasing pH. This may happen due to the increased OH⁻ ion concentration as they compete with fluoride ions for adsorption sites on the adsorbent surface²⁸. Another aspect is that; at higher pH, the adsorbent surface becomes negatively charged due to higher OH⁻ ions resulting in the increased repulsive forces between fluoride and hydroxide ions¹⁹. Similar results are observed in many studies which have used kaolin and eggshell powder in the literature^{15,19,20,27,44}.

3.3.4 Effect of initial concentration

The adsorption capacity increased with the increasing initial concentration as shown in Figure 9. The adsorption capacity of 0.06 mg/g shown at 5 mg/L was increased up to 0.71 mg/g at an initial concentration of 100 mg/L. This is because of the fact that the number of collisions between fluoride ions and the adsorbent functional groups also increases with the increase of initial fluoride concentration¹². Also, the increasing concentration gradient may create the necessary driving force to overcome the resistance of the mass transfer of fluoride between aqueous and solid phases which leads to an increased adsorption³⁴. Similar results have been reported in studies of fluoride removal by eggshells^{34,36}, kaolin²⁷, and also carbon nanotubes⁵¹.

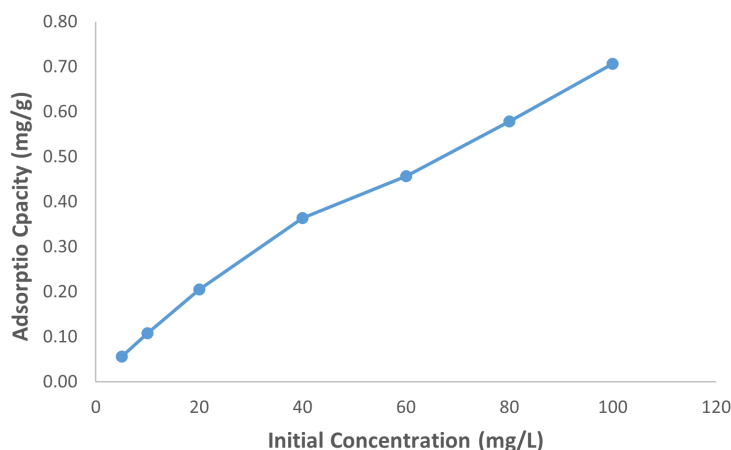


Figure 9. Effect of initial concentration on adsorption capacity for fluoride

3.4 Kinetic studies

The kinetic studies were carried out in order to investigate the kinetic mechanism that controls the adsorption process of CKE₃ using pseudo-first-order and pseudo-second-order models.

The pseudo-first-order kinetic model equation³⁰;

$$\log(q_e - q_t) = \log q_e - \frac{k_1}{2.303}t \quad (5)$$

where q_e and q_t are the amounts of fluoride adsorbed at equilibrium and at time t , in mg/g and k_1 is the first-order rate constant (min^{-1}).

The plot of “ $\log(q_e - q_t)$ ” versus “ t ” was constructed using the experimental data as shown in Figure 10. The pseudo-first-order rate constant (k_1) and the equilibrium adsorption capacity (q_e) were determined respectively from the slope and the intercept of the plot.

The pseudo-second-order kinetic model equation³⁰;

$$\frac{t}{q_t} = \frac{1}{k_2 q_e^2} + \frac{1}{q_e}t \quad (6)$$

where q_e is the equilibrium adsorption capacity for pseudo-second-order adsorption in mg/g and k_2 is the pseudo-second-order constant (g/mg/min).

The plot of “ t/q_t ” versus “ t ” was constructed using the experimental data, as shown in Figure 11. The pseudo-second-order rate constant (k_2) and the equilibrium adsorption capacity (q_e) were determined respectively from the intercept and

the slope of the plot. The calculated parameters of the pseudo-first order and pseudo-second order models are presented in Table 2.

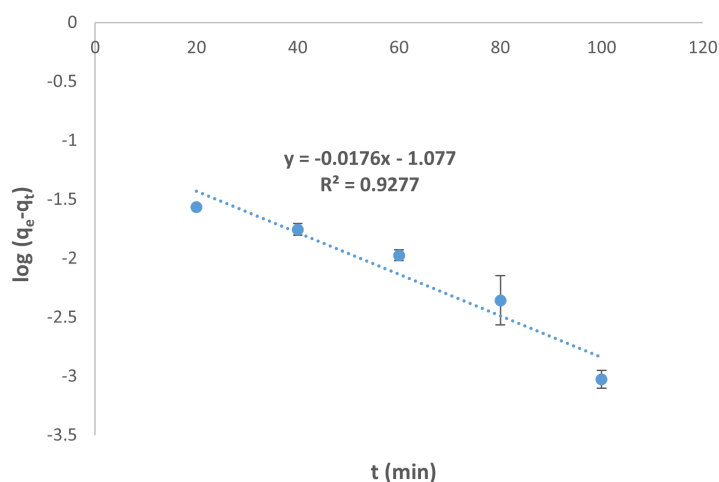


Figure 10. Pseudo-first-order kinetics

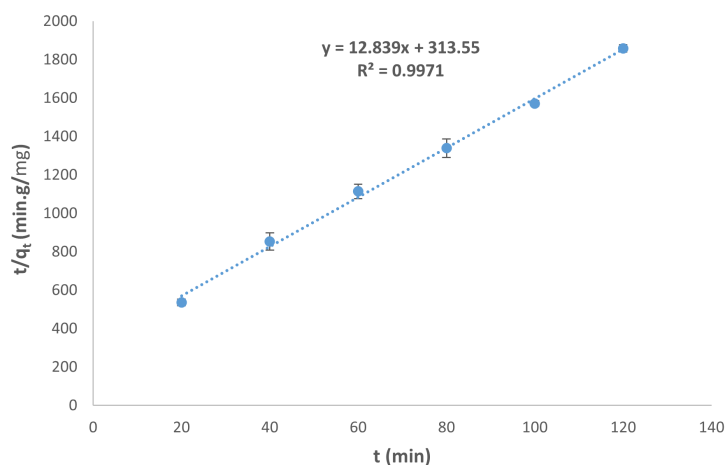


Figure 11. Pseudo-second-order kinetics

Table 2. Kinetic parameters for adsorption of fluoride onto CKE₃

First-Order Kinetic Model			Second-Order Kinetic Model		
q_e (mg/g)	k_1 (1/min)	R^2	q_e (mg/g)	k_2 (g/mg/min)	R^2
0.084	0.0405	0.928	0.078	0.524	0.997

Pseudo-second-order showed a higher linearity with a correlation coefficient (R^2) of 0.997 when compared to that of pseudo-first-order's 0.928. Also, the equilibrium adsorption capacity (q_e) calculated from the pseudo-second-order model is more close to the experimental q_e than the calculated q_e from the pseudo-first-order. Therefore pseudo-second-order model is considered to be more fitted for the fluoride adsorption of CKE₃. This suggests that the adsorption process of

fluoride onto CKE₃ could be chemisorption³⁴. This is in agreement with many previous fluoride removal studies done using eggshell powder^{19,33,34} and kaolin^{44,49}.

3.5 Isotherm studies

The isotherm studies were conducted in order to understand and interpret the adsorption mechanism of fluorides onto CKE₃ adsorbent. Langmuir and Freundlich isotherms were used in this study to evaluate the mechanism. The Langmuir isotherm explains the surface coverage by maintaining a balance between the relative rates of adsorption and desorption (dynamic equilibrium) while the Freundlich isotherm expresses the surface heterogeneity and the exponential distribution of active sites and their energies⁴¹.

The linearized Langmuir isotherm³⁰;

$$\frac{1}{q_e} = \frac{1}{q_m K_L C_e} + \frac{1}{q_m} \quad (7)$$

where q_e (mg/g) is the equilibrium adsorption capacity, q_m (mg/g) is the maximum adsorption capacity to form a complete monolayer on the surface, K_L (L/mg) is an adsorption equilibrium constant related to the affinity of the binding sites and energy of adsorption, and C_e (mg/L) is the equilibrium fluoride concentration of the solution.

The plot of “ $1/q_e$ ” versus “ $1/C_e$ ” was constructed using the experimental data as shown in Figure 12. Maximum adsorption capacity (q_m) and Langmuir constant K_L were determined from the intercept and the slope of the plot.

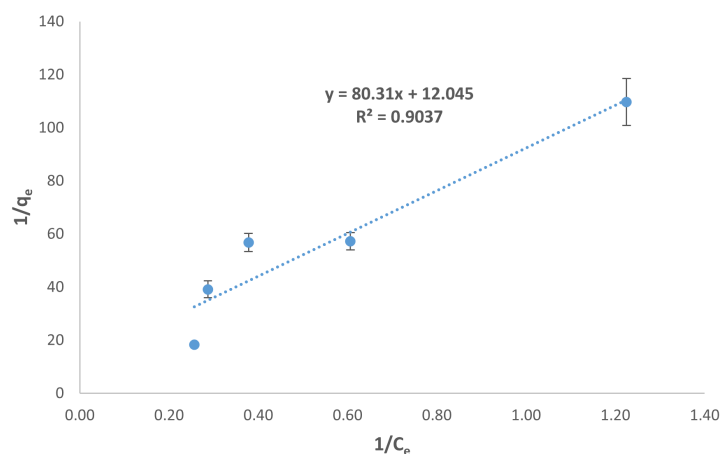


Figure 12. Langmuir isotherm for fluoride adsorption onto CKE₃

The linearized Freundlich isotherm³⁰;

$$\log q_e = \log K_F + \left(\frac{1}{n}\right) \log C_e \quad (8)$$

where q_e (mg/g) is the equilibrium adsorption capacity, C_e (mg/L) is the equilibrium fluoride concentration of the solution, K_F (mg/g)(mg/L)ⁿ or (mg/g (L/mg)^{1/n}) is a constant (Freundlich coefficient) indicative of adsorption capacity, and the dimensionless constant $1/n$ indicates the intensity of the adsorption or surface heterogeneity.

The plot of “ $\log q_e$ ” versus “ $\log C_e$ ” was constructed using the experimental data as shown in Figure 13. Freundlich constants K_F and n were determined from the intercept and the slope of the plot.

Table 3 shows the calculated parameters for Langmuir and Freundlich isotherms.

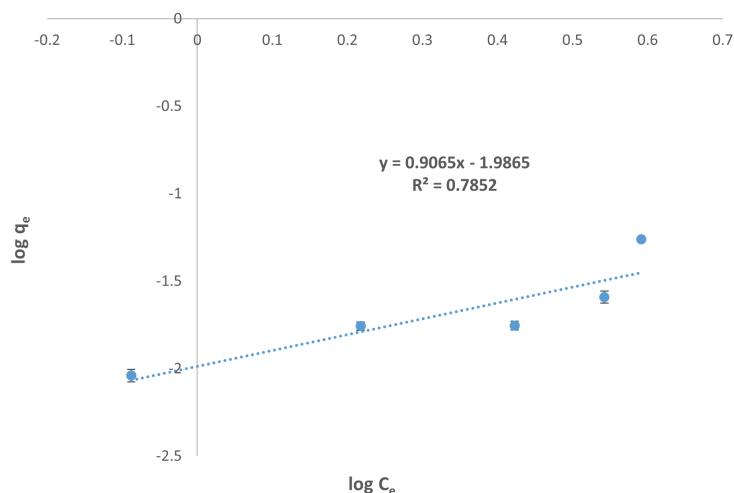


Figure 13. Freundlich isotherm for fluoride adsorption onto CKE₃

Table 3. Isotherm parameters for adsorption of fluoride onto CKE₃

Langmuir Model			Freundlich Model			
q_{max} (mg/g)	K_L (L/mg)	R^2	K_F	$1/n$	n	R^2
0.083	0.1500	0.904	0.0103	0.9065	1.10	0.785

The correlation coefficient (R^2) of Langmuir isotherm was 0.904, which is larger than R^2 of Freundlich isotherm ($R^2 = 0.785$). Therefore, Langmuir isotherm comparatively shows the best fitness for the adsorption mechanism of fluoride onto CKE₃. This suggests that the adsorption process is characterized by monolayer adsorption¹². Similar results were shown in fluoride removal studies which were done using Eggshell powder³⁴, Thermally treated eggshells¹⁹, alumina-supported eggshell composite¹⁵, Eggshell powder/chitosan nanofibers³⁶ and calcined kaolin/hydroxyapatite powders²⁸. The maximum monolayer adsorption capacity was found to be 0.083 mg/g and the adsorption equilibrium constant (K_L) was 0.15 L/mg.

In the Freundlich isotherm model, $1/n$ is a function of the strength of adsorption during the adsorption process¹⁹. In particular, sorption data correlation has made extensive use of the linear least-squares method and linearly transformed equations, where $1/n$ is a heterogeneity parameter and the smaller $1/n$, the higher the expected heterogeneity. When $1/n = 1$, this expression reduces to a linear adsorption isotherm. A favourable sorption process is indicated if n is between one and ten⁴⁰. In this study, the value of n was between 1 and 10 and $1/n$ was less than 1. Therefore, the adsorption process can be classified as favourable and the value of $1/n$ being close to 1 depicts a lower heterogeneity which suggests the better fitness for monolayer adsorption.

Therefore, considering the results of kinetics and isotherm studies, the mechanism of fluoride adsorption likely involves chemisorption, forming a monolayer on the adsorbent's surface through either surface complexation or ion exchange, with the adsorption being limited to the availability of active sites. At low concentrations fluoride is mainly removed by surface adsorption via electrostatic interactions, while at higher concentrations surface precipitation as CaF₂ is prominent⁵². Electrostatic interactions may have formed with active sites in both kaolinite and eggshell powder (see Table 4).

Table 4. Comparison of fluoride adsorption capacity with other reported low-cost-adsorbents

Material	q_{max} (mg/g)	Reference
Kaolin clay	0.070	53
Eggshell powder	0.052	33
Kaolin-bentonite composites adsorbents	0.047	48
Kaolin-bentonite composite	0.035	48
Calcined kaolin and eggshell powder composite	0.083	Present Study

In this study, a maximum adsorption capacity of 0.083 mg/L was observed, which demonstrates a promising potential compared to individual studies using eggshell powder and kaolin. Therefore, composite of eggshell and kaolin exhibits significant efficacy in fluoride removal from water. Furthermore, the formation of pellets enhances the practicality of its application.

3.6 Quality analysis of the CKE_3 treated water sample and mitigation actions for lowering the calcium ion interference

Water samples treated with 1 g of CKE_3 for one hour were analyzed for residual Calcium content and total hardness. The total hardness of the CKE_3 -treated water sample was 264 mg/L, while Calcium ion content was 196 mg/L. Pellets were washed with distilled water, dried and tested for fluoride removal. Likewise, one-time-washed pellets ($OCKE_3$) and two-time-washed pellets ($TCKE_3$) were analyzed for adsorption capacity under the same conditions used for CKE_3 . The adsorption capacities were 0.051 mg/g and 0.049 mg/g respectively for $OCKE_3$ and $TCKE_3$ (see Table 5).

Table 5. Calcium and total hardness levels of treated water

Adsorbent	Calcium Content as Ca (mg/L)	Total Hardness as $CaCO_3$ (mg/L)
CKE_3	196	264
$OCKE_3$	48	72
$TCKE_3$	24	60

* $OCKE_3$ —One-time-washed pellets, $TCKE_3$ —Two-time-washed pellets

From the results of this study, it is observed that the use of distilled water-washed pellets has significantly reduced the residual calcium content in the treated water and they are also under the stipulated levels. Also, the adsorbent capacity has not changed drastically. Therefore, $OCKE_3$ can be used for adsorption instead of CKE_3 to get the treated samples with lower calcium levels.

4. Conclusions

The results of this study showed that kaolin and eggshell blend is a potential adsorbent material for fluoride removal. The thermal treatment at 950 °C transformed kaolinite into metakaolinite, enhancing the stability of kaolin and rendering it suitable for pellet formation. The calcined kaolin pellets showed improved stability in water and the impregnation of eggshell powder enhanced the adsorption capacity of the adsorbent. Pseudo-second-order kinetic model and the Langmuir isotherm demonstrated greater suitability in explaining fluoride adsorption onto CKE_3 with a q_{max} of 0.083 mg/L. In conclusion, CKE_3 is a promising eco-friendly, low-cost adsorbent for the removal of fluoride from groundwater. Furthermore, this approach of development of the adsorbent as pellets is showcased by its simplicity and ease of application, rendering it highly suitable for practical utilization.

Acknowledgement

The authors thank the Department of Chemistry, University of Kelaniya, Sri Lanka and the Instrument Center, University of Sri Jayawardenepura, Sri Lanka for providing facilities for this study.

Conflict of interest

The authors declare that there are no conflict of interest.

References

- [1] Amini, H.; et al. Spatial and Temporal Variability of Fluoride Concentrations in Groundwater Resources of Larestan and Gerash Regions in Iran from 2003 to 2010. *Environ. Geochem. Health* **2016**, *38*, 25–37. <https://doi.org/10.1007/s10653-015-9676-1>.
- [2] Kimambo, V.; Bhattacharya, P.; Mtalo, F.; Mtamba, J.; Ahmad, A. Groundwater for Sustainable Development Fluoride Occurrence in Groundwater Systems at Global Scale and Status of de Fluoridation—State of the Art. *Groundw. Sustain. Dev.* **2019**, *9*, 100223. <https://doi.org/10.1016/j.gsd.2019.100223>.
- [3] Suneetha, M.; Sundar, B. S.; Ravindhranath, K. Groundwater Pollution and Adverse Effects on Health by Fluoride Ions. *J. Chem. Pharm. Res.* **2015**, *7*, 292–305.
- [4] Vithanage, M.; Bhattacharya, P. Fluoride in Drinking Water: Health Effects and Remediation. In *CO₂ Sequestration, Biofuels and Depollution; Environmental Chemistry for a Sustainable World*; Springer Nature: Cham, Switzerland, 2015; volume 5, pp. 105–151. https://doi.org/10.1007/978-3-319-11906-9_4.
- [5] Mukherjee, I.; Singh, U. K. Groundwater Fluoride Contamination, Probable Release, and Containment Mechanisms: A Review on Indian Context. *Environ. Geochem. Health* **2018**, *40*, 2259–2301. <https://doi.org/10.1007/s10653-018-0096-x>.
- [6] Farooqi, A. Arsenic and Fluoride Pollution in Water and Soils. In *Arsenic and Fluoride Contamination*; Springer: New Delhi, India, 2015; pp. 1–20. https://doi.org/10.1007/978-81-322-2298-9_1.
- [7] Rao, K.; Metre, M. Effective Low Cost Adsorbents for Removal of Fluoride from Water: A Review. *Int. J. Sci. Res.* **2014**, *3*, 1–5. <https://doi.org/10.21275/02014140>.
- [8] Srivastava, S.; Flora, S. J. S. Fluoride in Drinking Water and Skeletal Fluorosis: A Review of the Global Impact. *Curr. Environ. Heal. Rep.* **2020**, *7*, 140–146. <https://doi.org/10.1007/s40572-020-00270-9>.
- [9] Fawell, J.; Bailey, K.; Chilton, J.; Dahi, E.; Fewtrell, L.; Magara, Y. *Fluoride in Drinking-Water-WHO*; IWA Publishing: London, UK, 2006.
- [10] Bhatnagar, A.; Kumar, E.; Sillanpää, M. Fluoride Removal from Water by Adsorption-A Review. *Chem. Eng. J.* **2011**, *171*, 811–840. <https://doi.org/10.1016/j.cej.2011.05.028>.
- [11] Mohapatra, M.; Anand, S.; Mishra, B. K.; Giles, D. E.; Singh, P. Review of Fluoride Removal from Drinking Water. *J. Environ. Manage.* **2009**, *91*, 67–77. <https://doi.org/10.1016/j.jenvman.2009.08.015>.
- [12] Vinati, A.; Mahanty, B.; Behera, S. K. Clay and Clay Minerals for Fluoride Removal from Water: A State-of-the-Art Review. *Appl. Clay Sci.* **2015**, *114*, 340–348. <https://doi.org/10.1016/j.clay.2015.06.013>.
- [13] Yadav, K. K.; Gupta, N.; Kumar, V.; Khan, S. A.; Kumar, A. A Review of Emerging Adsorbents and Current Demand for Defluoridation of Water: Bright Future in Water Sustainability. *Environ. Int.* **2018**, *111*, 80–108. <https://doi.org/10.1016/j.envint.2017.11.014>.
- [14] Vijaya, Y.; Krishnaiah, A. Sorptive Response Profile of Chitosan Coated Silica in the Defluoridation of Aqueous Solution. *E-Journal Chem.* **2009**, *6*, 713–724. <https://doi.org/10.1155/2009/748153>.
- [15] Lunge, S.; Thakre, D.; Kamble, S.; Labhsetwar, N.; Rayalu, S. Alumina Supported Carbon Composite Material with Exceptionally High Defluoridation Property from Eggshell Waste. *J. Hazard. Mater.* **2012**, *237–238*, 161–169. <https://doi.org/10.1016/j.jhazmat.2012.08.023>.
- [16] Daifullah, A. A. M.; Yakout, S. M.; Elreefy, S. A. Adsorption of Fluoride in Aqueous Solutions Using KMnO₄-Modified Activated Carbon Derived from Steam Pyrolysis of Rice Straw. *J. Hazard. Mater.* **2007**, *147*, 633–643. <https://doi.org/10.1016/j.jhazmat.2007.01.062>.

- [17] Batistella, L.; Venquiaruto, L. D.; Di Luccio, M.; Oliveira, J. V.; Pergher, S. B. C.; Mazutti, M. A.; De Oliveira, D.; Mossi, A. J.; Treichel, H.; Dallago, R. Evaluation of Acid Activation under the Adsorption Capacity of Double Layered Hydroxides of Mg-Al-CO₃ Type for Fluoride Removal from Aqueous Medium. *Ind. Eng. Chem. Res.* **2011**, *50*, 6871–6876. <https://doi.org/10.1021/ie101020r>.
- [18] Ayalew, A. A. Development of Kaolin Clay as a Cost-Effective Technology for Defluoridation of Groundwater. *Int. J. Chem. Eng.* **2020**, *2020*, 8820727. <https://doi.org/10.1155/2020/8820727>.
- [19] Lee, J. I.; Hong, S. H.; Lee, C. G.; Park, S. J. Fluoride Removal by Thermally Treated Egg Shells with High Adsorption Capacity, Low Cost, and Easy Acquisition. *Environ. Sci. Pollut. Res.* **2021**, *28*, 35887–35901. <https://doi.org/10.1007/s11356-021-13284-z>.
- [20] Meenakshi, S.; Sundaram, C. S.; Sukumar, R. Enhanced Fluoride Sorption by Mechanochemically Activated Kaolinites. *J. Hazard. Mater.* **2008**, *153*, 164–172. <https://doi.org/10.1016/j.jhazmat.2007.08.031>.
- [21] Vivek Vardhan, C. M.; Srimurali, M. Removal of Fluoride from Water Using a Novel Sorbent Lanthanum-Impregnated Bauxite. *Springerplus* **2016**, *5*. <https://doi.org/10.1186/s40064-016-3112-6>.
- [22] Basu, H.; Singhal, R. K.; Pimple, M. V.; Reddy, A. V. R. Synthesis and Characterization of Alumina Impregnated Alginate Beads for Fluoride Removal from Potable Water. *Water Air Soil Pollut.* **2013**, *224*. <https://doi.org/10.1007/s11270-013-1572-7>.
- [23] Gebrewold, B. D.; Kijjanapanich, P.; Rene, E. R.; Lens, P. N. L.; Annachhatre, A. P. Fluoride Removal from Groundwater Using Chemically Modified Rice Husk and Corn Cob Activated Carbon. *Environ. Technol.* **2018**, *40*, 2913–2927. <https://doi.org/10.1080/09593330.2018.1459871>.
- [24] Vhangwele, M.; Mugeru, G. W.; Tholiso, N. Defluoridation of Drinking Water Using Al³⁺-Modified Bentonite Clay: Optimization of Fluoride Adsorption Conditions. *Toxicol. Environ. Chem.* **2014**, *96*, 1294–1309. <https://doi.org/10.1080/02772248.2014.977289>.
- [25] Gitari, W. M.; Ngulube, T.; Masindi, V.; Gumbo, J. R. Defluoridation of Groundwater Using Fe³⁺-Modified Bentonite Clay: Optimization of Adsorption Conditions. *Desalination Water Treat.* **2013**, *53*, 1578–1590. <https://doi.org/10.1080/19443994.2013.855669>.
- [26] Koutník, P.; Soukup, A.; Bezucha, P.; Šafář, J.; Hájková, P.; Čmelík, J. Comparison of Kaolin and Kaolinitic Claystones as Raw Materials for Preparing Metakaolinite-Based Geopolymers. *Ceram. Silikaty* **2019**, *63*, 110–123. <https://doi.org/10.13168/cs.2019.0003>.
- [27] Lugwisha, E. H. Water Defluoridation Capacity of Tanzanian Kaolin-Feldspar Blend Adsorbents. *Am. J. Appl. Chem.* **2016**, *4*, 77. <https://doi.org/10.11648/j.ajac.20160403.12>.
- [28] Laonapakul, T.; Suthi, T.; Otsuka, Y.; Mutoh, Y.; Chaikool, P.; Chindaprasirt, P. Fluoride Adsorption Enhancement of Calcined-Kaolin/Hydroxyapatite Composite. *Arab. J. Chem.* **2022**, *15*, 104220. <https://doi.org/10.1016/j.arabjc.2022.104220>.
- [29] Biswas, K.; Gupta, K.; Goswami, A.; Ghosh, U. C. Fluoride Removal Efficiency from Aqueous Solution by Synthetic Iron(III)-Aluminum(III)-Chromium(III) Ternary Mixed Oxide. *Desalination* **2010**, *255*, 44–51. <https://doi.org/10.1016/j.desal.2010.01.019>.
- [30] Akafu, T.; Chimdi, A.; Gomoro, K. Removal of Fluoride from Drinking Water by Sorption Using Diatomite Modified with Aluminum Hydroxide. *J. Anal. Methods Chem.* **2019**, *2019*, 4831926. <https://doi.org/10.1155/2019/4831926>.
- [31] Mittal, A.; Teotia, M.; Soni, R. K.; Mittal, J. Applications of Egg Shell and Egg Shell Membrane as Adsorbents: A Review. *J. Mol. Liq.* **2016**, *223*, 376–387. <https://doi.org/10.1016/j.molliq.2016.08.065>.
- [32] Santos, A. F.; Arim, A. L.; Lopes, D. V.; Gando-Ferreira, L. M.; Quina, M. J. Recovery of Phosphate from Aqueous Solutions Using Calcined Eggshell as an Eco-Friendly Adsorbent. *J. Environ. Manage.* **2019**, *238*, 451–459. <https://doi.org/10.1016/j.jenvman.2019.03.015>.
- [33] Assami, Z.; Messaitfa, A. Use of Eggshell as a Low-Cost Alternative Adsorbent for Elimination of Fluoride from Groundwater. *Pollution* **2023**, *9*, 39–55. <https://doi.org/10.22059/poll.2022.341026.1425>.
- [34] Bhaumik, R.; Mondal, N. K.; Das, B.; Roy, P.; Pal, K. C.; Das, C.; Banerjee, A.; Datta, J. K. Eggshell Powder as an Adsorbent for Removal of Fluoride from Aqueous Solution: Equilibrium, Kinetic and Thermodynamic Studies. *E-Journal Chem.* **2012**, *9*, 1457–1480. <https://doi.org/10.1155/2012/790401>.
- [35] Kashi, G.; Mehree, A.; Zaeimdar, M.; Khoshab, F.; Mohades Madaree, A. Removal of Fluoride from Urban Drinking Water by Eggshell Powder. *Bulg. Chem. Commun.* **2015**, *47*, 187–192.

- [36] Abbasi, A.; Memon, S. A.; Qureshi, R. F.; Mehdi, M.; Khatri, M.; Ahmed, F.; Khatri, Z.; Kim, I. S. Adsorptive Defluoridation from Aqueous Solution Using a Novel Blend of Eggshell Powder and Chitosan Nanofibers. *Mater. Res. Express* **2020**, *7*. <https://doi.org/10.1088/2053-1591/abcd6e>.
- [37] Nor, N. M.; Kamil, N. H. N.; Mansor, A. I.; Maarof, H. I. Adsorption Analysis of Fluoride Removal Using Graphene Oxide/Eggshell Adsorbent. *Indones. J. Chem.* **2020**, *20*, 579–586. <https://doi.org/10.22146/ijc.43481>.
- [38] Nathan, A. J.; Scobell, A. APHA AWWA 23rd EDITION. *Foreign Aff.* **2017**, *91*, 1689–1699.
- [39] Mohadi, R.; Anggraini, K.; Riyanti, F.; Lesbani, A. Preparation Calcium Oxide From Chicken Eggshells. *Sriwij. J. Environ.* **2016**, *1*, 32–35. <https://doi.org/10.22135/sje.2016.1.2.32-35>.
- [40] Amarasinghe, A.; Wanniarachchi, D. Eco-Friendly Photocatalyst Derived from Egg Shell Waste for Dye Degradation. *J. Chem.* **2019**, *2019*, 8184732. <https://doi.org/10.1155/2019/8184732>.
- [41] Ayawei, N.; Ebelegi, A. N.; Wankasi, D. Modelling and Interpretation of Adsorption Isotherms. *J. Chem.* **2017**, *2017*, 3039817. <https://doi.org/10.1155/2017/3039817>.
- [42] Dewi, R.; Agusnar, H.; Alfian, Z.; Tamrin. Characterization of Technical Kaolin Using XRF, SEM, XRD, FTIR and Its Potentials as Industrial Raw Materials. *J. Phys. Conf. Ser.* **2018**, *1116*, 042010. <https://doi.org/10.1088/1742-6596/1116/4/042010>.
- [43] Kumar, A.; Lingfa, P. Sodium Bentonite and Kaolin Clays: Comparative Study on Their FT-IR. *Mater. Today Proc.* **2020**, *22*, 737–742. <https://doi.org/10.1016/j.matpr.2019.10.037>.
- [44] Ayalew, A. A. Comparative Adsorptive Performance of Adsorbents Developed from Kaolin Clay and Limestone for De-Fluoridation of Groundwater. *South Afr. J. Chem. Eng.* **2023**, *44*, 1–13. <https://doi.org/10.1016/j.sajce.2022.11.002>.
- [45] Liu, Y.; Lei, S.; Lin, M.; Li, Y.; Ye, Z.; Fan, Y. Assessment of Pozzolan Activity of Calcined Coal-Series Kaolin. *Appl. Clay Sci.* **2017**, *143*, 159–167. <https://doi.org/10.1016/j.clay.2017.03.038>.
- [46] Wang, H.; Li, C.; Peng, Z. Characterization and Thermal Behavior of Kaolin. *J. Therm. Anal. Calorim.* **2011**, *105*, 157–160. <https://doi.org/10.1007/s10973-011-1385-0>.
- [47] Cree, D.; Rutter, A. Sustainable Bio-Inspired Limestone Eggshell Powder for Potential Industrialized Applications. *ACS Sustain. Chem. Eng.* **2015**, *3*, 941–949. <https://doi.org/10.1021/acssuschemeng.5b00035>.
- [48] Annan, E.; Nyankson, E.; Agyei-Tuffour, B.; Armah, S. K.; Nkrumah-Buandoh, G.; Hodasi, J. A. M.; Oteng-Peprah, M. Synthesis and Characterization of Modified Kaolin-Bentonite Composites for Enhanced Fluoride Removal from Drinking Water. *Adv. Mater. Sci. Eng.* **2021**, *2021*, 6679422. <https://doi.org/10.1155/2021/6679422>.
- [49] Nabbou, N.; Belhachemi, M.; Boumelik, M.; Merzougui, T.; Lahcene, D.; Harek, Y.; Zorpas, A. A.; Jeguirim, M. Removal of Fluoride from Groundwater Using Natural Clay (Kaolinite): Optimization of Adsorption Conditions. *Comptes Rendus Chim.* **2019**, *22*, 105–112. <https://doi.org/10.1016/j.crci.2018.09.010>.
- [50] Mahvi, A. H.; Heibati, B.; Mesdaghinia, A.; Yari, A. R. Fluoride Adsorption by Pumice from Aqueous Solutions. *E-Journal Chem.* **2012**, *9*, 1843–1853. <https://doi.org/10.1155/2012/581459>.
- [51] Balarak, D.; Mahdavi, Y.; Bazrafshan, E.; Mahvi, A. H.; Esfandyari, Y. Adsorption of Fluoride from Aqueous Solutions by Disorders and Diseases Have Been Identified Associated with the Excess Intake of F⁻ such as Dental and Skeletal Fluorosis, Infertility, Brain Damage, and Thyroid This Study Was Conducted on a Laboratory. *Fluoride* **2016**, *49*, 71–83.
- [52] Budyanto, S.; Kuo, Y. L.; Liu, J. C. Adsorption and Precipitation of Fluoride on Calcite Nanoparticles: A Spectroscopic Study. *Sep. Purif. Technol.* **2015**, *150*, 325–331. <https://doi.org/10.1016/j.seppur.2015.07.016>.
- [53] Mumtaz, N.; Pandey, G.; Labhasetwar, P. K. Global Fluoride Occurrence, Available Technologies for Fluoride Removal, and Electrolytic Defluoridation: A Review. *Crit. Rev. Environ. Sci. Technol.* **2015**, *45*, 2357–2389. <https://doi.org/10.1080/10643389.2015.1025638>.

Supplementary Material

Supplementary Material can be available at: <https://ojs.wiserpub.com/index.php/UJGC/article/view/4962/2600>.